Available online at www.sciencedirect.com

ScienceDirect

Ceramics International 40 (2014) 9249–9256

CERAMICS INTERNATIONAL

www.elsevier.com/locate/ceramint

Preparation and multiferroic properties of 2-2 type $CoFe_2O_4/Pb(Zr,Ti)O_3$ composite films with different structures

Min Shi, Ruzhong Zuo, Yudong Xu*, Lei Wang, Cang Gu, Hailin Su, Jiagang Zhong, Guiyang Yu

Institute of Electro Ceramics & Devices, School of Materials Science and Engineering, Hefei University of Technology, Hefei 230009, China

Received 9 January 2014; received in revised form 30 January 2014; accepted 31 January 2014
Available online 14 February 2014

Abstract

2-2 Type layered CFO/PZT ($CoFe_2O_4/Pb(Zr_{0.52}Ti_{0.48})O_3$) magnetoelectric composite films with four different structures were prepared on $Pt/Ti/SiO_2/Si$ substrates via a sol–gel method. These films annealed at 700 °C contain PZT and CFO phase without impurity phases. The prepared composite films exhibit 2-2 type layered structures with obvious interfaces and no diffusions exist between CFO and PZT films. Ferromagnetic and ferroelectric responses were simultaneously observed in the composite films. These composite films exhibit good magnetoelectric coupling effects and the magnetoelectric voltage coefficients (α_E) increase with increasing the volume contents of CFO films in composite films. The α_E value of composite film (2PZT/4CFO/2PZT/4CFO/2PZT) reaches a maximum (227 mV cm^{-1} Oe^{-1}) among all the prepared composite films.

Keywords: C. Ferroelectric properties; Ferromagnetic properties; Magnetoelectric coupling effect; 2-2 Type composite films

1. Introduction

It is well-known that the multiferroic materials exhibit magnetoelectric (ME) coupling effect between the ferroelectric and ferromagnetic phases apart from the conventional ferroelectric and ferromagnetic properties. The ME coupling effect is a spontaneous electric polarization induced by an external magnetic field [1–5], which is usually characterized by ME voltage coefficient α_E (α_E=dE/dH, where E is the induced electric field and H is the applied magnetic field [4]). Multiferroic materials are of great concern owing to their attractive multi-functional features and potential applications in multi-functional devices such as transducers, actuators, and sensors [6–9]. Nowadays, it is well recognized that the ME coupling effect actually arises from the mechanical interactions which originate from the magnetostrictive and piezoelectric effects in individual phases of magnetoelectric composite films [10–12]. In order to fabricate the composite films with enhanced ME coupling effect, ferromagnetic phases with large magnetostrictive effect and ferroelectric phases with large piezoelectric effect should be needed [8,10]. Owing to a greater magnetostrictive coefficient of $CoFe_2O_4$ (CFO) and a greater piezoelectric coefficient of $Pb(Zr_xTi_{1-x})O_3$ (PZT), CFO/PZT composite films have stimulated extensive interests [13–16]. However, the applications of the magnetoelectric composite films for multi-functional devices are still limited due to their weak magnetoelectric coupling effects. Consequently, various research groups have been trying to improve the magnetoelectric coupling properties of the composite films [13,16,17].

Generally speaking, the multiferroic composite films have three different structures including 0-3 type, 1-3 type, and 2-2 type [4]. It is found that ME voltage coefficients cannot be directly measured in 0-3 and 1-3 structured films owing to a leakage problem, which results from the low resistance of the ferromagnetic phase in the ferroelectric matrix [4]. In addition, it is not very easy to control growths of the composite films with 0-3 or 1-3 type structures [18]. Noticeably, the leakage currents of ME composite films with 2-2 type or layered structures can be significantly reduced by isolating the low resistive ferromagnetic layers with insulating ferroelectric layers [12]. And it is easy to control the growth of composite films with 2-2 type structures [19,20]. Therefore, the 2-2 type

*Corresponding author. Tel./fax: +86 551 62901363.
E-mail address: mrshimin@hotmail.com (Y.D. Xu).

http://dx.doi.org/10.1016/j.ceramint.2014.01.146
0272-8842

composite films have become potential candidates for magnetoelectric applications. Wan et al. [21] and Ortega et al. [22] deposited the multilayer ferroelectric and ferromagnetic film on the substrate successively in order to prepare 2-2 type PZT/CFO composite films, which were unexpectedly changed to 0-3 type films after being annealed [21,22]. This may be due to the diffusions between the PZT and CFO films in the composite films, implying that it is more difficult to prepare the PZT/CFO composite films with 2-2 type structures. Recently, a lot of researches have been dedicated to the

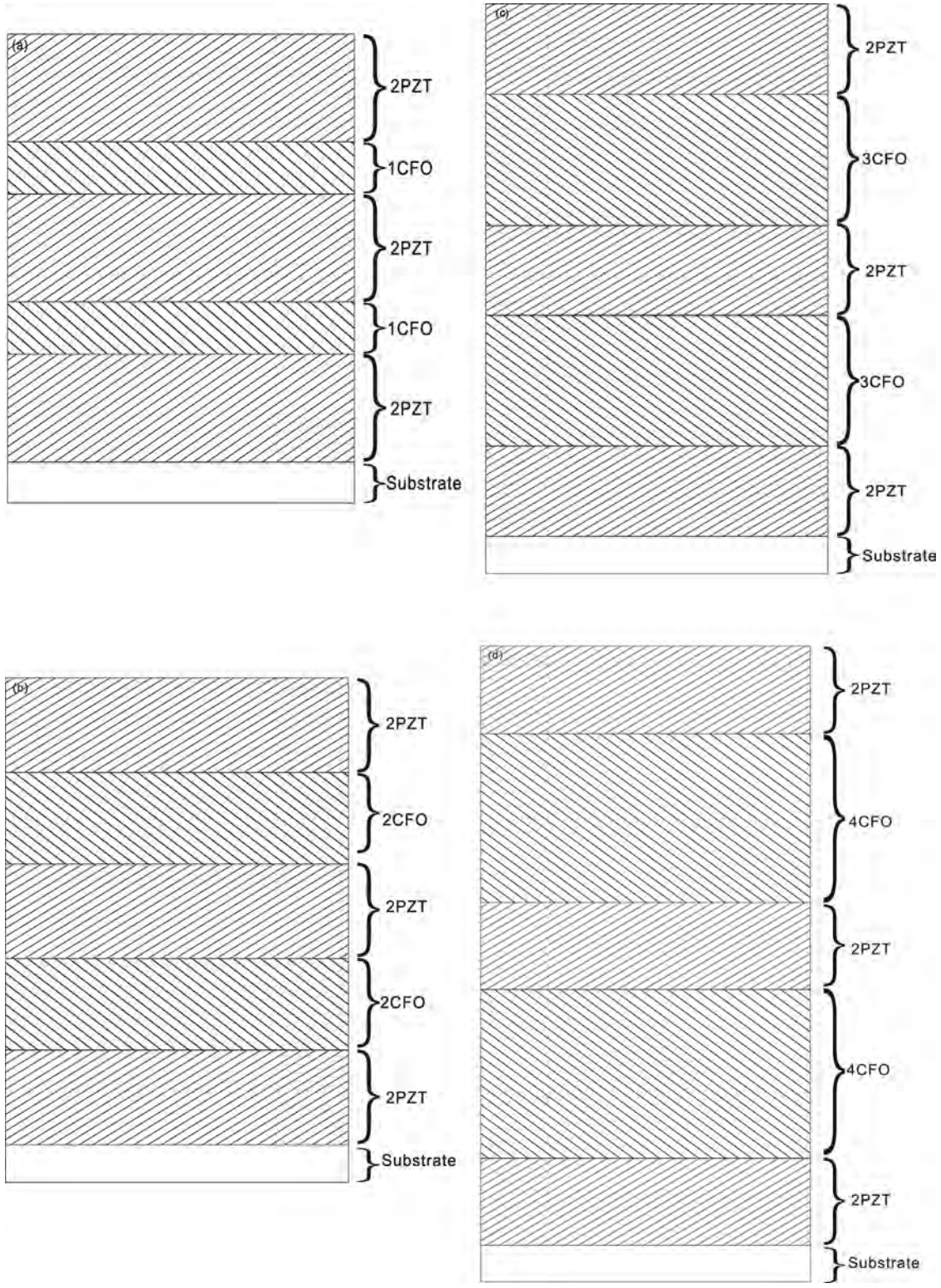

Fig. 1. Schematic diagrams of CFO/PZT composite films with different thicknesses of CFO films; (a) $P_2C_1P_2C_1P_2$, (b) $P_2C_2P_2C_2P_2$, (c) $P_2C_3P_2C_3P_2$ and (d) $P_2C_4P_2C_4P_2$.

preparation of ME multilayer films, however, up to now, few reports on the relationships among the structures and ferroelectric, ferromagnetic properties, ME properties of the composite films are available [23,24].

In this work, the CFO/PZT composite films with 2-2 type structures were prepared on the substrate (Pt/Ti/SiO_2/Si) via a sol–gel process and spin-coating technique. The composite films have clear interfaces between CFO and PZT phases. No impurity phases were found in the prepared composite films. In addition, the authors also investigated the relationships between the structures and properties of the composite films by modifying the volume contents of CFO films in the composite films, with the aim to obtain 2-2 type composite materials with high ME coupling effects.

2. Experimental

Iron nitrate ($Fe(NO_3)_3 \cdot 9H_2O$), cobalt nitrate ($Co(NO_3)_2 \cdot 6H_2O$) and citric acid ($C_6H_8O_7 \cdot H_2O$) were firstly dissolved into anhydrous alcohol to form a mixed solution. The molar ratio of Fe^{2+}:Co^{2+}:$C_6H_8O_7$ was 2:1:6. After the solution was stirred for 5 h at 60 °C, the anhydrous alcohol was added to obtain 0.15 mol/L CFO sol solution. Then, it was continuously stirred for 2 h and placed at room temperature for 24 h to form a stable CFO precursor solution.

Tetrabutyl titanate ($Ti(C_4H_9O)_4$) and zirconium nitrate pentahydrate ($Zr(NO_3)_4 \cdot 5H_2O$) were dissolved into 2-methoxyethanol separately to obtain two kinds of solutions. Lead acetate trihydrate ($Pb(CH_3COO)_2 \cdot 3H_2O$) was dissolved into glacial acetic acid ($CH_3(COOH)_2$) to obtain a solution. The above-mentioned three kinds of solutions were firstly mixed. Then, $Zr(NO_3)_4 \cdot 5H_2O$ solution was added to obtain a homogeneous solution. The molar ratio of Pb^{2+}:Zr^{4+}:Ti^{4+} was 1.1:0.52:0.48 (excessive 10 mol% Pb^{2+} is required to compensate the loss of lead during annealing). 2-Methoxyethanol was added to obtain the PZT sol solution (0.30 mol/L), which was stirred and heated at 60 °C for 24 h to obtain a stable precursor solution of PZT. The precursor solution was yellowish and clear.

The precursor solution of PZT was spin-coated on the substrate (Pt/Ti/SiO_2/Si) at a spinning rate of 3000 rpm for 30 s. Then, the gel film was dried at 140 °C for 2 min. This spin-coating/drying procedure was repeated several times until the required two-layered PZT films were obtained. The PZT films were annealed at different temperatures for 10 min. The preparation processes of CFO films were similar to those of PZT films.

In order to prepare the composite films, the PZT starting precursor solution was spin-coated on the substrate (Pt/Ti/SiO_2/Si) and dried. This spin-coating/drying procedure was repeated two times to obtain PZT films with two layers. The films were annealed at 700 °C for 10 min. Then, the CFO starting precursor solution was spin-coated on the PZT films and dried. This spin-coating/drying procedure was repeated different times to obtain CFO films with different layer numbers according to the structures of the composite films. The films were also annealed at 700 °C for 10 min. The final composite films were prepared by repeating the above process. In order to investigate the relationships between the structures of multilayered films and the multiferroic properties, the authors prepared the composite film with the structure, 2PZT/1CFO/2PZT/1CFO/2PZT (abbreviated as $P_2C_1P_2C_1P_2$, where P stands for PZT films, C stands for CFO films, the number in the subscript stands for the spin-coating repeating times) firstly. Subsequently, three composite films with structures of $P_2C_2P_2C_2P_2$, $P_2C_3P_2C_3P_2$ and $P_2C_4P_2C_4P_2$ were prepared for comparison. The schematic diagram of CFO/PZT composite films with different structures is shown in Fig. 1. The authors are able to investigate how the volume contents of the CFO films in the composite films can influence the multiferroic properties of the composite films by fixing the thicknesses of PZT films in the composite films.

The CFO and PZT precursor solutions were dried at 80 °C in an oven to obtain powders. The phase compositions and crystallographic structures of the powders and composite films were performed by using an X-ray diffraction (D/Max-rB, Rigaku, Japan) with CuKα radiation. The surface and cross-section morphologies of the CFO, PZT and composite films were observed with a field-emission scanning electron microscope (Sirion200, FEI, USA). The ferromagnetic behaviors of the CFO and composite films were detected by a vibration sample magnetometer (BHV-55, Riken, Japan). The ferroelectric behaviors of the PZT and composite films were characterized by using a ferroelectric tester (Precision LC, Radiant Technologies, USA). Magnetoelectric effects of the composite films were measured by using a self-designed magnetoelectric measuring device. Ag electrodes with a diameter of 150 μm were deposited through a shadow mask on the PZT and composite films before testing the ferroelectric and magnetoelectric properties.

3. Results and discussion

Fig. 2 depicted X-ray diffraction (XRD) patterns of CFO powders annealed at different temperatures. It illustrates that powders annealed at 550 °C contain more amount of impurity phase (Fe_2O_3) except the main phase (CFO). With increasing annealing temperature, the relative amount of impurity phase decreases remarkably. It is apparent that there is no detectable secondary phase when the annealing temperature reaches

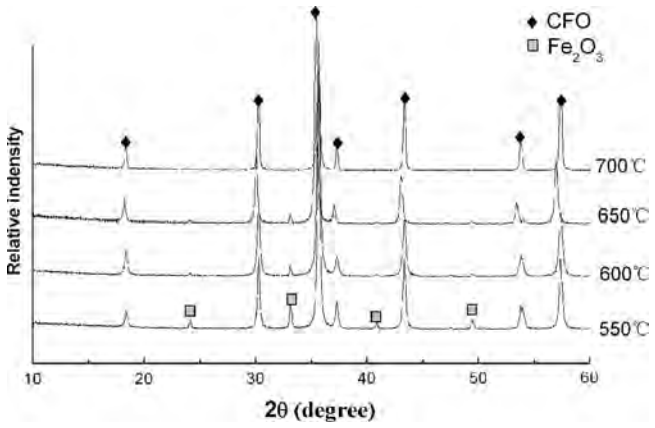

Fig. 2. XRD patterns of CFO powders annealed at different temperatures.

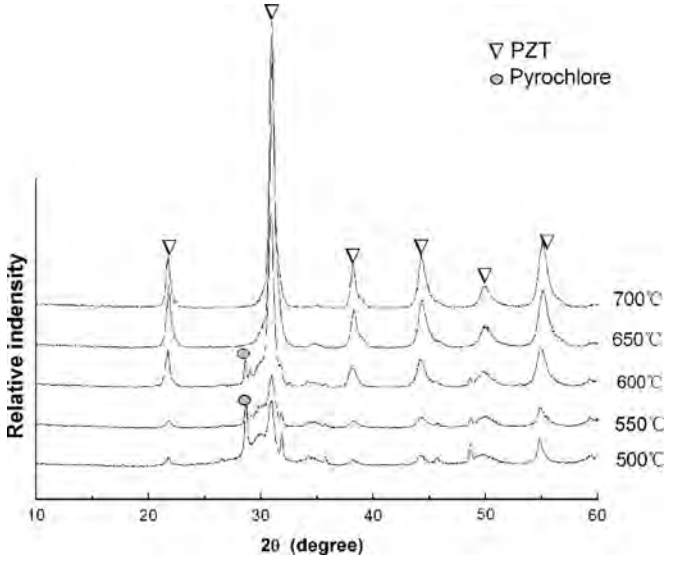

Fig. 3. XRD patterns of PZT powders annealed at different temperatures.

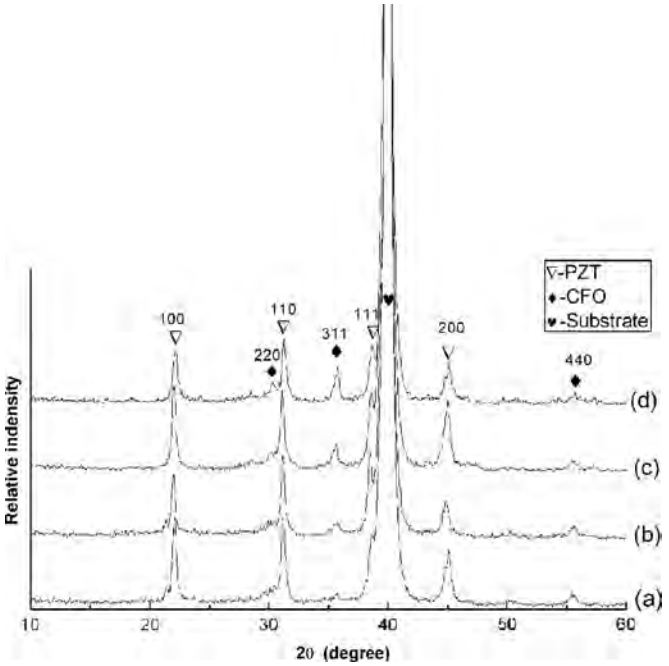

Fig. 4. XRD patterns of the composite films with different layer numbers of CFO films annealed at 700 °C for 10 min; (a) $P_2C_1P_2C_1P_2$, (b) $P_2C_2P_2C_2P_2$, (c) $P_2C_3P_2C_3P_2$ and (d) $P_2C_4P_2C_4P_2$.

700 °C. Consequently, the lowest annealing temperature of CFO is 700 °C. Fig. 3 shows X-ray diffraction (XRD) results of the PZT powders annealed at different temperatures. It shows that the PZT powders annealed at 500 °C are composed of the main phase (PZT phase) and more amount of secondary phase, i.e. pyrochlore. The relative amount of pyrochlore decreases with increasing annealing temperatures. It is apparent that there is no detectable secondary phase when the temperature is increased to 650 °C. Consequently, the lowest annealing temperature of PZT is 650 °C. Based on the results of XRD, CFO and PZT films should be annealed at 700 °C and 650 °C to assure the formation of pure phases, respectively. Therefore the annealing temperature of the composite films was set at 700 °C to ensure the formation of pure CFO and PZT phases. Fig. 4 demonstrates XRD patterns of the CFO/PZT composite films with different layer structures annealed at 700 °C. For all of the four composite films, they are all composed of PZT and CFO phases apart from Pt phase from the substrate, with no impurity phases. It is consistent with the XRD results of CFO and PZT powders. It also shows that the PZT and CFO phases can separate from each other completely without forming intermediate phases, which is important for the composite films to possess greater ME coupling effects [25]. It can also be seen that the CFO and PZT films in the composite films have polycrystalline structures and the composite films do not exhibit preferentially crystallographic orientation. It is also observed that the crystallinity of PZT film is higher than that of CFO film. This may be due to the fact that the crystallization temperature of PZT film is lower than that of CFO film [11].

Fig. 5 shows SEM image of surface of one-layered CFO film. It shows that the film has compact structure and small amount of cracks without any pore. Fig. 6 shows SEM image of cross section of one-layered CFO film. It is seen that the thickness of CFO film is about 49.0 nm. Noticeably, the accurate interface between the CFO film and substrate is

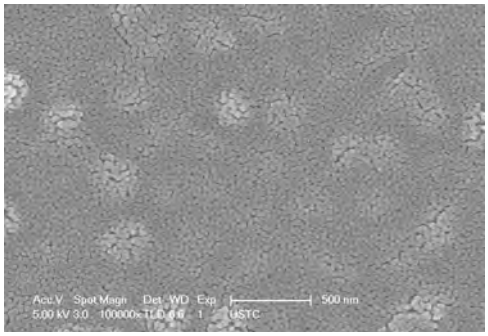

Fig. 5. SEM image of surface of one-layered CFO film.

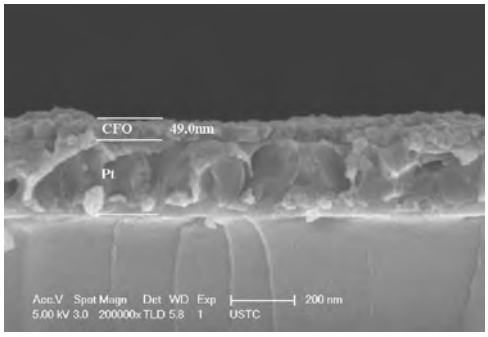

Fig. 6. SEM image of cross-section of one-layered CFO film.

difficult to identify, implying that the diffusion between the CFO film and substrate may occur. Fig. 7 shows SEM image of surface of two-layered PZT film. It demonstrates that the

film has even grains without cracks and pores. Fig. 8 shows SEM image of cross section of two-layered PZT film. The thickness of two-layered PZT film is 97.0 nm. Average thickness of single layered PZT film is 48.5 nm. The interface between PZT film and substrate is clear and flat. No transition layer is observed. This indicates that there is no obvious diffusion between PZT film and substrate. Based on the SEM results of the CFO and PZT film, the PZT film, not the CFO film, was first deposited on the substrate in order to avoid the diffusion between the film and substrate. PZT film deposited on the substrate can also act as a buffer layer to reduce the restraint of the substrate to the strain of the film and improve the ME coupling effects of the composite films [13,26].

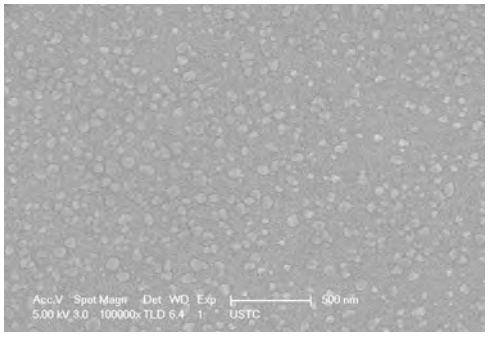

Fig. 7. SEM image of surface of two-layered PZT films.

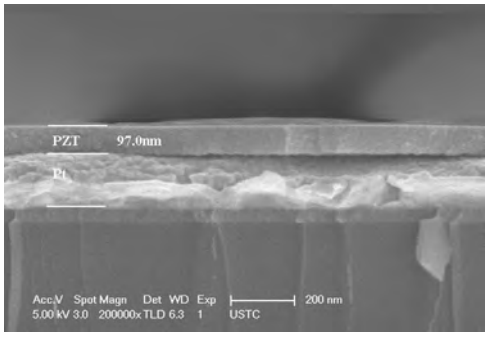

Fig. 8. SEM image of cross-section of two-layered PZT films.

The SEM cross-sectional images of the CFO/PZT composite films with four different layered structures are shown in Fig. 9. It is seen that all of the four composite films have 2-2 type layered structures other than 0-3 or 1-3 type structures. The composite films are dense and well crystallized. It also indicated that the composite films have obvious interface between CFO and PZT film without forming transition layer. This implies that there is no obvious diffusion between the CFO and PZT phase. It will be helpful to reduce the leakage in the composite films and therefore improve the ME coupling effects of the composite films [27]. It also reveals that the four composite films have layered or 2-2 type structures, not 0-3 type structures. For these composite films, the film thicknesses of PZT and CFO films, volume contents of CFO films are listed in Table 1. From Table 1, it is clear that, with increasing the thicknesses of CFO films in the composite films, the volume contents of CFO films in composite films increase. The volume contents of CFO films will greatly affect the ferroelectric, ferromagnetic and magnetoelectric properties of the composite films, which will be discussed later.

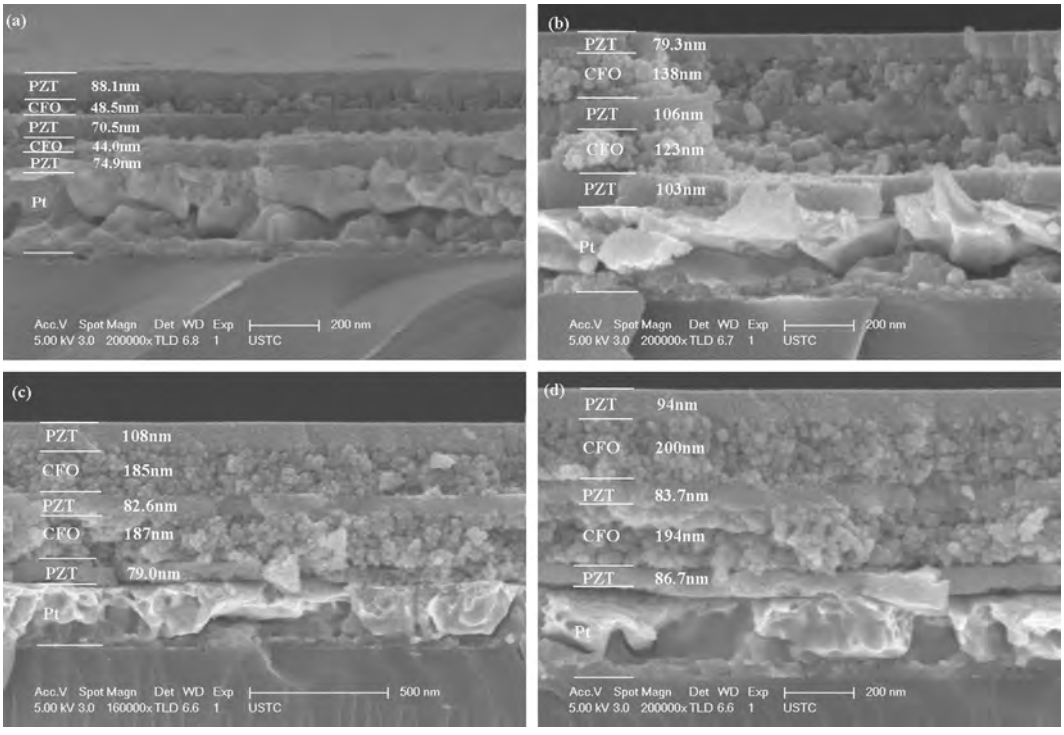

Fig. 9. SEM cross-sectional images of the composite films with different thickness of CFO films annealed at 700 °C for 10 min; (a) $P_2C_1P_2C_1P_2$, (b) $P_2C_2P_2C_2P_2$, (c) $P_2C_3P_2C_3P_2$ and (d) $P_2C_4P_2C_4P_2$.

Table 1
The thicknesses of the CFO and PZT films, volume contents of CFO films in the CFO–PZT composite films.

Type of composite films	The corresponding film thicknesses (nm)	Volume contents of CFO films (%)
$P_2C_1P_2C_1P_2$	88.1, 48.5, 70.5, 44.0, 74.9	28.4
$P_2C_2P_2C_2P_2$	79.3, 138.0, 106.0, 123.0, 103.0	47.5
$P_2C_3P_2C_3P_2$	108.0, 185.0, 82.6, 187.0, 79.0	58.0
$P_2C_4P_2C_4P_2$	94.0, 200.0, 83.7, 194.0, 86.7	59.8

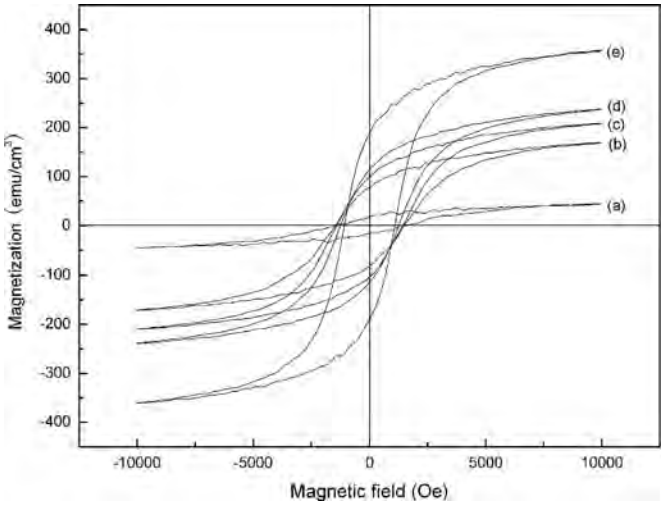

Fig. 10. Magnetic hysteresis loops of the composite films with different thickness of CFO films and the pure CFO film annealed at 700 °C for 10 min; (a) $P_2C_1P_2C_1P_2$, (b) $P_2C_2P_2C_2P_2$, (c) $P_2C_3P_2C_3P_2$, (d) $P_2C_4P_2C_4P_2$ and (e) pure CFO film.

Table 2
The ferromagnetic parameters of the CFO–PZT composite films and pure CFO film.

Films	Volume contents of CFO films (%)	M_r (emu cm^{-3})	H_c (Oe)
Composite films ($P_2C_1P_2C_1P_2$)	28.4	18.80	1667.91
Composite films ($P_2C_2P_2C_2P_2$)	47.5	78.07	1510.99
Composite films ($P_2C_3P_2C_3P_2$)	58.0	99.72	1458.66
Composite films ($P_2C_4P_2C_4P_2$)	59.8	113.62	1262.43
Pure CFO film	100.0	187.19	1092.36

Magnetic hysteresis loops of pure CFO film and four composite films are presented in Fig. 10. It is clear that the five magnetic hysteresis loops exhibit obvious ferromagnetic properties and reach the saturated state. The results drawn from Fig. 10 are listed in Table 2. It is also seen that the remanent magnetizations (M_r) of the composite films increase with increasing the volume contents of CFO films in the compose films. The reason is that the M_r values of the composite films are mainly determined by the relative amount of ferromagnetic phase [28]. The M_r value of the composite film ($P_2C_4P_2C_4P_2$) reaches the maximum (113.62 emu/cm^3), which is much lower than that of pure CFO film (187.19 emu/cm^3). This may be due to the smaller volume contents of CFO phases in the composite

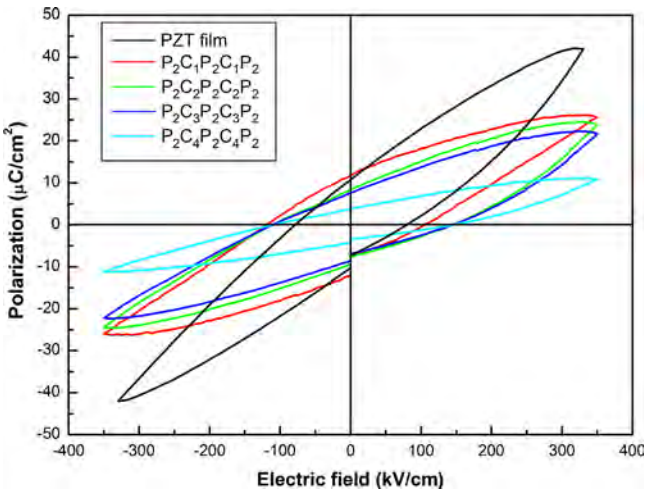

Fig. 11. *P–E* hysteresis loop of the pure PZT film and the composite films annealed at 700 °C for 10 min, testing at 100 Hz.

films than that in pure CFO film. In addition, the coercive magnetic fields (H_c) of composite films decrease with increasing the volume contents of the CFO films. This may be attributed to the magnetostatic interactions between adjacent CFO films [13]. The H_c values of the composite films are greater than that of pure CFO films (1092.36 Oe). The reason may be that the substrate can restrict the rotation of magnetic domain and, therefore, the H_c values of the composite films will be enhanced [27].

Fig. 11 shows polarization–electric field (*P–E*) hysteresis loop of the four composite films and pure PZT film at room temperature. The results drawn from Fig. 11 are listed in Table 3. It is clearly seen that the remanent polarizations (P_r) of the composites decrease with increasing the volume contents of CFO films. This may be due to the dilute influence of ferromagnetic phases on the composite films [4]. The P_r value of the composite film ($P_2C_4P_2C_4P_2$) reaches a minimum (3.54 μC cm^{-2}), which is much lower than that of pure PZT films (P_r=11.01 μC cm^{-2}). However, the coercive electric fields (E_c) of the other three composite films are very close except that of the composite film ($P_2C_1P_2C_1P_2$). The reason is not clear now. The E_c values of composite films are much greater than that of pure PZT film (81.59 kV cm^{-1}). This may be attributed to the influence of CFO phase with comparatively high conductivity [4].

The variations of α_E with magnetic bias (H_{bias}) for the four composite films are shown in Fig. 12. It is clear that these composite films exhibit significant ME coupling properties which depend on H_{bias}. With increasing H_{bias}, the α_E values of the four composite films increase quickly, reach maximum when H_{bias} is near 460 Oe, then decrease. It should be noted that the α_E values of the four composite films increase with increasing the volume contents of CFO films at the same H_{bias}. For ME coupling effects mainly arise from the magnetic–mechanical–electric transformations through the stress-mediated transfers in the interfaces of the composite films [10,11], therefore increasing volume contents of CFO phases with low H_c values and high magnetostrictions will be of help

Table 3
The ferroelectric parameters of the CFO–PZT composite films and pure PZT film.

Films	Volume contents of CFO films (%)	P_r (μC cm^{-2})	E_c (kV cm^{-1})
Composite films ($P_2C_1P_2C_1P_2$)	28.4	11.01	106.93
Composite films ($P_2C_2P_2C_2P_2$)	47.5	8.66	146.83
Composite films ($P_2C_3P_2C_3P_2$)	58.0	7.54	147.23
Composite films ($P_2C_4P_2C_4P_2$)	59.8	3.54	147.55
Pure PZT film	0	11.31	81.59

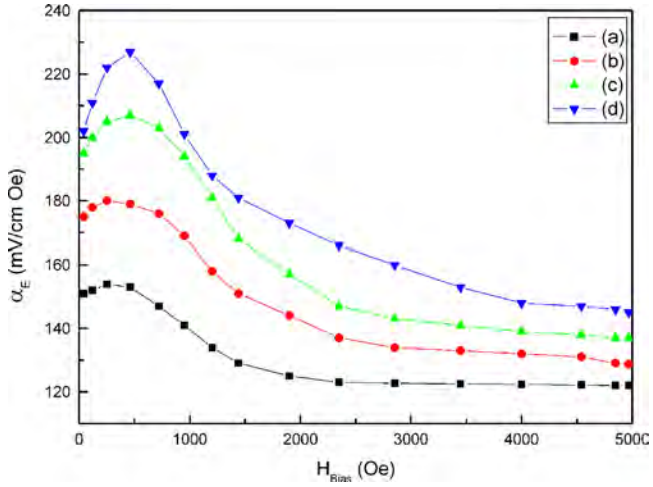

Fig. 12. Variations of α_E with H_{bias} for the CFO/PZT composite film annealed at 700 °C for 10 min; (a) $P_2C_1P_2C_1P_2$, (b) $P_2C_2P_2C_2P_2$, (c) $P_2C_3P_2C_3P_2$ and (d) $P_2C_4P_2C_4P_2$.

to improve ME coupling effects of the composite films [29]. Moreover, the maximum of α_E (227 mV cm^{-1} Oe^{-1}) was found in the composite film ($P_2C_4P_2C_4P_2$), which is much greater than those reported in Ref. [30] (35 mV cm^{-1} Oe^{-1}) and Ref. [31] (155 mV cm^{-1} Oe^{-1}).

4. Conclusions

2-2 Type CFO/PZT composite films with four different volume contents of CFO films were deposited on substrates (Pt/Ti/SiO_2/Si) by sol–gel method and spin-coating technique. The composite films have not only ferromagnetic and ferroelectric, but also magnetoelectric coupling properties. When annealed at 700 °C, the four composite films are composed of CFO, PZT phase and Pt phase from the substrate without impurity phases. The four composite films exhibit 2-2 type layered structures with obvious interfaces between CFO and PZT films. There is no obvious diffusion between CFO and PZT films in the composite films. With increasing the volume contents of CFO films in composite films, the M_r values of the CFO/PZT composite films increase, the H_c and P_r values decrease. However, the E_c values of the composite films do not change obviously except that of the composite film ($P_2C_1P_2C_1P_2$).

The four composite films exhibit magnetoelectric effects. The α_E values of the composite films increase with increasing the volume contents of the CFO films in composite films. The maximum of α_E, 227 mV cm^{-1} Oe^{-1}, was observed in the composite film ($P_2C_4P_2C_4P_2$), which is much greater than those of other's results. The ME composite films with high values of α_E will be attractive for technological applications.

Acknowledgment

This work was supported by Anhui Provincial Natural Science Foundation (1308085ME59), Nippon Sheet Glass Foundation for Materials Science and Engineering of Japan (2012QTXM0079), the National Natural Science Foundation of China (51272060).

References

[1] R.C. Kambale, D. Patil, J. Ryu, Y.S. Chai, K.H. Kim, W.H. Yoon, D.Y. Jeong, D.S. Park, J.W. Kim, J.J. Choi, C.W. Ahn, Colossal magnetoelectric response of PZT thick films on Ni substrates with a conductive $LaNiO_3$ electrode, J. Phys. D: Appl. Phys. 46 (2013) 092002–092005.
[2] J. Ma, J. Hu, Z. Li, C.W. Nan, Recent progress in multiferroic magnetoelectric composites: from bulk to thin films, Adv. Mater. 23 (2011) 1062–1067.
[3] D. Patil, J.H. Kim, Y.S. Chai, J.H. Nam, J.H. Cho, B.I. Kim, K.H. Kim, Large longitudinal magnetoelectric coupling in $NiFe_2O_4$–$BaTiO_3$ laminates, Appl. Phys. Express 4 (2011) 073001–073003.
[4] A. McDannald, M. Staruch, G. Sreenivasulu, C. Cantoni, G. Srinivasan, Magnetoelectric coupling in solution derived 3-0 type $PbZr_{0.52}Ti_{0.48}O_3$: $x CoFe_2O_4$ nanocomposite films, Appl. Phys. Lett. 102 (2013) 122905–122905-4.
[5] G. Srinivasan, Magnetoelectric composites, Annu. Rev. Mater. Res. 40 (2010) 153–178.
[6] C.P. Cheng, M.H. Tang, X.S. Lv, Z.H. Tang, Y.G. Xiao, Magnetoelectric coupling in $La_{0.6}Ca_{0.4}MnO_3$–$Bi_{0.6}Nd_{0.4}TiO_3$ composite thin films derived by a chemical solution deposition method, Appl. Phys. Lett. 101 (2012) 212902–212903.
[7] W. Eerenstein, N.D. Mathur1, J.F. Scott, Multiferroic and magnetoelectric materials, Nature 442 (2006) 759–765.
[8] T.D. Cheng, X.G. Tang, Y. Wang, H.L.W. Chan, Strong magnetoelectric coupling in sol–gel derived multiferroic $(Pb_{0.76}Ca_{0.24})TiO_3$–$CoFe_2O_4$ composite films, Solid State Sci. 14 (2012) 1492–1495.
[9] L. Zhang, J.W. Zhai, W.F. Mo, X. Yao, Electric and magnetic properties of $(x)CoFe_2O_4$–$(1-x)BaTiO_3$ thick film prepared by electrophoretic deposition technique, Solid State Sci. 13 (2011) 321–325.
[10] L. Zhang, J.W. Zhai, W.F. Mo, X. Yao, Doping effect on crystal structure of $BaTiO_3$ and magnetoelectric coupling of layered composites $Tb_{1-x}Dy_xFe_{2-y}$–$BaTi_{0.99}M_{0.01}O_{3+\delta}$, J. Alloys Compd. 472 (2009) 257–261.
[11] S.H. Xie, Y.M. Liu, Y. Ou, Q.N. Chen, X.L. Tan, J.Y. Li, Magnetoelectric coupling of multilayered $Pb(Zr_{0.52}Ti_{0.48})O_3$–$CoFe_2O_4$ film by

piezoresponse force microscopy under magnetic field, J. Appl. Phys. 112 (2012) 074110–074115.
[12] C.W. Nan, Magnetoelectric effect in composites of piezoelectric and piezomagnetic phases, Phys. Rev. B 50 (1994) 6082–6088.
[13] Y.D. Xu, L. Wang, M. Shi, H.L. Su, G. Wu, Magnetostatic coupling in $CoFe_2O_4$/$Pb(Zr_{0.53}Ti_{0.47})O_3$ magnetoelectric composite thin films of 2-2 type structure, Chin. J. Chem. Phys. 25 (2012) 115–119.
[14] S.H. Xie, J.Y. Li, Y. Qiao, Y.Y. Liu, L.N. Lan, Y.C. Zhou, S.T. Tan, Multiferroic $CoFe_2O_4$–$Pb(Zr_{0.52}Ti_{0.48})O_3$ nanofibers by electrospinning, Appl. Phys. Lett. 92 (2008) 06290–06293.
[15] H.C. He, J.P. Zhou, J. Wang, C.W. Nan, Multiferroic $Pb(Zr_{0.5}2Ti_{0.48})O_3$–$Co_{0.9}Zn_{0.1}Fe_2O_4$ bilayer thin films via a solution processing, Appl. Phys. Lett. 89 (2006) 052904–052904-3.
[16] C. Cibert, J. Zhu, G. Poullain, R. Bouregba, J. More-Chevalier, A. Pautrat, Magnetoelectric coupling in $Tb_{0.3}Dy_{0.7}Fe_2$/Pt/$PbZr_{0.56}Ti_{0.44}O_3$ thin films deposited on Pt/TiO_2/SiO_2/Si substrate, Appl. Phys. Lett. 102 (2013) 022906–022906-4.
[17] R. Rania, J.K. Juneja, S. Singhc, K.K. Rainad, C. Prakashe, Dielectric, ferroelectric, magnetic and magnetoelectric properties of $0.1Ni_{0.8}Zn_{0.2}$-Fe_2O_4–$0.9Pb_{1-3x/2}SmxZr_{0.65}Ti_{0.35}O_3$ magnetoelectric composites, Ceram. Int. 39 (2013) 7845–7851.
[18] C.W. Nan, M.I. Bichurin, S. Dong, D. Viehland, G. Srinivasan, Multiferroic magnetoelectric composites: historical perspective, status, and future directions, J. Appl. Phys. 103 (2008) 031101–031135.
[19] J. Wang, L. Wang, G. Liu, Z. Shen, Y. Lin, C.W. Nan, Substrate effect on the magnetoelectric behavior of $Pb(Zr_{0.5}2Ti_{0.48})O_3$ film-on-$CoFe_2O_4$ bulk ceramic composites prepared by direct solution spin coating, J. Am. Ceram. Soc. 92 (2009) 2654–2660.
[20] C.S. Park, A. Khachaturyan, S. Priya, Giant magnetoelectric coupling in laminate thin film structure grown on magnetostrictive substrate, Appl. Phys. Lett. 100 (2012) 192904–192904-4.
[21] J.G. Wan, X.W. Wang, Y.J. Wu, M. Zeng, Y. Wang, H. Jiang, W.Q. Zhou, G.H. Wang, J.M. Liu, Magnetoelectric $CoFe_2O_4$–Pb(Zr,Ti)O_3 composite thin films derived by a sol–gel process, Appl. Phys. Lett. 86 (2005) 122501–122503.
[22] N. Ortega, P. Bhattacharya, R.S. Katiyar, P. Dutta, A. Manivannan, M.S. Seehra, I. Takeuchi, S.B. Majumder, Multiferroic properties of Pb(Zr,Ti)O_3/$CoFe_2O_4$ composite thin films, J. Appl. Phys. 100 (2006) 126105–126105-3.
[23] T. Li, Z. Hu, M. Zhang, K. Li, D. Yu, H. Yan, Frequency dependence of magnetoelectric effect in epitaxial $La_{0.7}Sr_{0.3}MnO_3$/$BaTiO_3$ bilayer film, Appl. Surf. Sci. 258 (2012) 4558–4562.
[24] D. Zhou, G. Jian, Y. Zheng, S. Gong, F. Shi, Electrophoretic deposition of $BaTiO_3$/$CoFe_2O_4$ multiferroic composite films, Appl. Surf. Sci. 257 (2011) 7621–7626.
[25] L.Q. Weng, Y.D. Fu, S.H. Song, J.N. Tang, J.Q. Li, Synthesis of lead zirconate titanate–cobalt ferrite magnetoelectric particulate composites via an ethylenediaminetetraacetic acid-citrate gel process, J. Scr. Mater. 56 (2007) 465–468.
[26] W. Chen, Z.H. Wang, C. Ke, W. Zhu, O.K. Tan, Preparation and characterization of $Pb(Zr_{0.53}Ti_{0.47})O_3$/$CoFe_2O_4$ composite thick films by hybrid sol–gel processing, Mater. Sci. Eng. B 162 (2009) 47–52.
[27] Y.A. Wang, Y.B. Wang, W. Rao, J.X. Gao, W.L. Zhou, J. Yu, Electric and magnetic properties and magnetoelectric effect of the $Ba_{0.8}Sr_{0.2}TiO_3$/$CoFe_2O_4$ heterostructure film by radio-frequency magnetron sputtering, Chin. Phys. Lett. 30 (2013) 047502–047504.
[28] H.C. He, J. Ma, J. Wang, C.W. Nan, Orientation-dependent multiferroic properties in $Pb(Zr_{0.52}Ti_{0.48})O_3$–$CoFe_2O_4$ nanocomposite thin films derived by a sol–gel processing, J. Appl. Phys. 103 (2008) 034103–034105.
[29] L. Wang, R.Z. Zuo, H.L. Su, M. Shi, Y.D. Xu, G. Wu, G.Y. Yu, Processing and magneto-electric properties of sol–gel-derived Pb$(Zr_{0.52}Ti_{0.48})O_3$–$Ni_{0.8}Zn_{0.2}Fe_2O_4$ 2-2 type multilayered films, J. Mater. Sci. 46 (2011) 5394–5399.
[30] J.G. Wan, H. Zhang, X.W. Wang, D.Y. Pan, J.M. Liu, G.H. Wang, Magnetoelectric $CoFe_2O_4$-lead zirconate titanate thick films prepared by a polyvinylpyrrolidone-assisted sol–gel method, Appl. Phys. Lett. 89 (2006) 122914–122914-3.
[31] J. Wang, Z. Li, Y. Shen, Y.H. Lin, C.W. Nan, Enhanced magnetoelectric coupling in $Pb(Zr_{0.52}Ti_{0.48})O_3$ film-on-$CoFe_2O_4$ bulk ceramic composite with $LaNiO_3$ bottom electrode, J. Mater. Sci. 48 (2013) 1021–1026.